Published in final edited form as:

ACS Biomater Sci Eng. 2021 August 09; 7(8): 3908–3916. doi:10.1021/acsbiomaterials.1c00865.

Biodegradable, Tissue Adhesive Polyester Blends for Safe, Complete Wound Healing

John L. Daristotle[⊥],
Fischell Department of Bioengineering, University of Maryland, College Park, Maryland 20742, United States

Metecan Erdi[⊥],
Department of Chemical and Biomolecular Engineering, University of Maryland, College Park, Maryland 20742, United States

Lung W. Lau,
Sheikh Zayed Institute for Pediatric Surgical Innovation, Joseph E. Robert Jr. Center for Surgical Care, Children's National Medical Center, Washington, District of Columbia 20010, United States

Shadden T. Zaki,
Department of Materials Science and Engineering, University of Maryland, College Park, Maryland 20742, United States

Priya Srinivasan,
Sheikh Zayed Institute for Pediatric Surgical Innovation, Joseph E. Robert Jr. Center for Surgical Care, Children's National Medical Center, Washington, District of Columbia 20010, United States

Manogna Balabhadrapatruni,
Department of Chemical and Biomolecular Engineering, University of Maryland, College Park, Maryland 20742, United States

Omar B. Ayyub,
Department of Chemical and Biomolecular Engineering, University of Maryland, College Park, Maryland 20742, United States

Anthony D. Sandler,
Sheikh Zayed Institute for Pediatric Surgical Innovation, Joseph E. Robert Jr. Center for Surgical Care, Children's National Medical Center, Washington, District of Columbia 20010, United States

Peter Kofinas

Corresponding Author kofinas@umd.edu .
[⊥]J.L.D. and M.E. contributed equally to this manuscript.

Author Contributions

The manuscript was written through contributions of all authors. All authors have given approval to the final version of the manuscript.

The authors declare no competing financial interest.

ASSOCIATED CONTENT

Supporting Information

The Supporting Information is available free of charge at https://pubs.acs.org/doi/10.1021/acsbiomaterials.1c00865.

Histology of unwounded porcine skin tissue (Figure S1); gel permeation chromatography of low- and high-molecular-weight PLCL (Figure S2) and mass loss data for low- and high-molecular-weight PLCL (Figure S3) (PDF)

Department of Chemical and Biomolecular Engineering, University of Maryland, College Park, Maryland 20742, United States

Abstract

Pressure-sensitive adhesives typically used for bandages are nonbiodegradable, inhibiting healing, and may cause an allergic reaction. Here, we investigated the effect of biodegradable copolymers with promising thermomechanical properties on wound healing for their eventual use as biodegradable, biocompatible adhesives. Blends of low molecular weight (LMW) and high molecular weight (HMW) poly(lactide-*co*-caprolactone) (PLCL) are investigated as tissue adhesives in comparison to a clinical control. Wounds treated with PLCL blend adhesives heal completely with similar vascularization, scarring, and inflammation indicators, yet require fewer dressing changes due to integration of the PLCL adhesive into the wound. A blend of LMW and HMW PLCL produces an adhesive material with significantly higher adhesive strength than either neat polymer. Wound adhesion is comparable to a polyurethane bandage, utilizing conventional nonbiodegradable adhesives designed for extremely strong adhesion.

Graphical Abstract

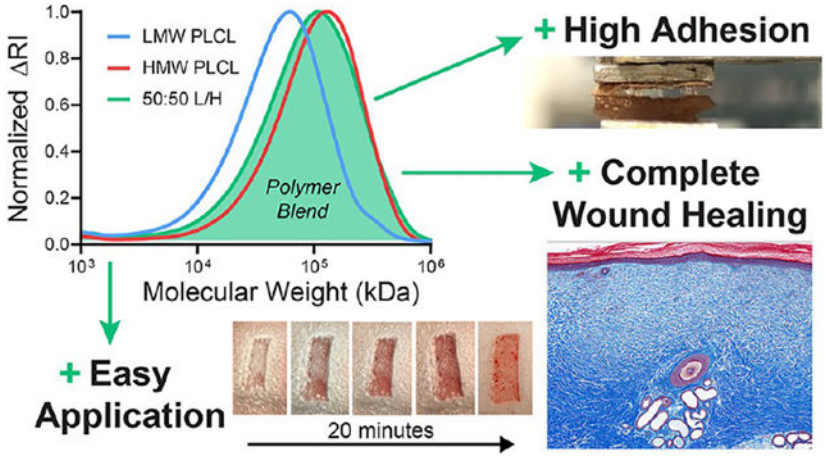

Keywords

tissue adhesion; wound healing; biodegradable adhesive; sprayable polymer; bandage

INTRODUCTION

Conformal bandages available both over-the-counter and exclusively in the clinic are coated with a pressure-sensitive adhesive (PSA). PSAs, which allow fixation to a surface simply by applying pressure to the interface without any curing event, are typically composed of acrylic, polyisobutylene (PIB), or poly(styrene-butadiene-styrene) (PSBS) block copolymers blended with a phenolic-tackifying resin of relatively low-molecular-weight (LMW).[1–3] While these synthetic rubber PSAs can adhere effectively to skin, which is dry and hydrophobic unlike the wet, hydrophilic tissue surfaces of internal organs, they are nondegradable, have been shown to cause allergic dermatitis, and may strip the healing

wound of newly deposited tissues.[4–6] Despite these challenges, synthetic rubber PSAs are widely used as adhesives for various medical devices, especially bandages and wound dressings.[7,8]

Advances in medical PSAs have focused on reducing damage to the healing wound during removal, developing switchable chemistries, improving water permeability, and using biologically derived materials. Silicone adhesives have been developed to prevent the adherence of healing skin tissues to the adhesive during bandage removal.[9–13] Responsive chemistries also allow for adhesion to be reduced on-demand, aiding in bandage removal. Various formulation changes have been made to improve water absorption, exudate control, and water transport.[14–16] Some biologically derived sugar-incorporating adhesives were developed for enhanced biocompatibility by accelerating biodegradation, although with limited effect due to having incorporated a nondegradable acrylic.[17,18] However, few of these developments have yielded demonstrable improvements to effectiveness in controlled preclinical trials, and useful applications of advanced wound dressings are dependent on specific characteristics of the wound.[19]

Biodegradable polyesters such as poly(lactic-*co*-glycolic acid) (PLGA) or poly(caprolactone) (PCL) have been used to create surgical sealants and other adhesive devices.[20–24] Most have the advantage of degrading completely into metabolites with low toxicity, making them superior to acrylic, PIB, or PSBS PSAs, which either do not degrade, release toxic byproducts, or have the potential to cause a harmful immune response. PSAs developed from a biodegradable polyester could be incorporated as the adhesive layer in conventional bandages, as a cost-effective replacement for typical PSAs, or could be used as a stand-alone spray to secure nonadhesive devices such as gauze. We have previously used solution blow spinning (SBS) to deposit tissue adhesive polymers from an organic solvent. In SBS, the volatile solvent evaporates during spraying, yielding a dry, conformal fiber mat, and cytotoxicity studies show that fibroblast cell viability is unaffected by the spraying solvent and process.[25,26] Herein, we used in vivo experiments with a porcine partial-thickness wound model and adhesive tests with ex vivo skin sections to demonstrate that blends of low and high molecular weight (HMW) poly(lactide-*co*-caprolactone) (PLCL) deposited via SBS could be used to create a sprayable and biodegradable PSA for various wound healing applications.

MATERIALS AND METHODS

Polymer Solutions for Producing Pressure-Sensitive Tissue Adhesives.

Polymer solutions were prepared at a 20% w/v concentration in acetone. Three polymer solutions were investigated: (1) a low-molecular-weight solution (LMW) consisting of poly(D,L-lactide-*co*-caprolactone) (70:30 L/CL, acid endcap, Mn 15 000–25 000 Da, Akina), (2) a high-molecular-weight (HMW) solution consisting of poly(D,L-lactide-*co*-caprolactone) (70:30 L/CL, acid endcap, Mn 35 000–45 000 Da, Akina), and (3) a polymer blend solution (denoted 50:50 L/H) containing a 50:50 mass ratio of LMW and HMW. An airbrush (Master Airbrush, G22-SET, 0.2 mm nozzle diameter) was used to deposit the tissue adhesives as dry, conformal polymer fibers. The airbrush was connected to a compressed CO_2 tank equipped with a pressure regulator set to 20 psig.

Mass Loss and Degradation Testing.

Unless stated otherwise, polymer samples were produced by solution blow spinning (SBS) onto a 22 mm by 22 mm glass coverslip, with the distance between the airbrush nozzle and coverslip at approximately 10 cm. Polymer samples for mass loss studies were produced by spraying 2 mL of polymer solution onto a coverslip. A microbalance (Sartorius ME-5) was used to determine the net increase in mass after the spinning process was complete, which is the initial sample mass, m_i. Samples were submerged in 4 mL of 1× phosphate-buffered saline (PBS) in wells of a 6-well plate and stored in a shaker incubator at 37 °C and 100 rpm. Samples were removed at time points of 1, 3, 7, and 14 days. At these points, the PBS was removed, and the samples were stored in a vacuum desiccator for 3 days. The samples were weighed again to determine the final mass, m_f, and mass loss ($m_i - m_f$) was calculated as a percentage of m_i. Samples that swell with water may produce a negative mass loss because of incomplete water removal and salt that remains in the polymer matrix. Five samples were used for each time point and polymer composition ($n = 5$).

Gel Permeation Chromatography.

Polymer samples from time points of degradation (1, 3, 7, 14 days) and nondegraded samples (0 days) were dissolved at 3 mg mL^{-1} in tetrahydrofuran (THF). Samples were run on the Waters e2695 Separations Module with a Waters 2414 Refractive Index Detector and Waters HSPgel columns in series (HR MB-Land HR 3.0 columns, 6.0 mm i.d. × 15 cm). Molecular weight is reported as polystyrene relative molecular weight, as calculated from a 10-point calibration curve generated using Agilent EasiCal polystyrene standards dissolved at 2 mg mL^{-1} in THF. GPC analysis was performed using Waters Empower 3 Chromatography Data software. The weight-average molecular weight, number-average molecular weight, and polydispersity of each sample were then obtained from the sample curves and recorded. Each sample type was replicated 3 times ($n = 3$).

Differential Scanning Calorimetry (DSC).

Polymer samples were sealed in aluminum hermetic pans (TA Instruments) using a sample encapsulation press. DSC measurements were made on a TA Instruments DSC Q100. Samples were held isothermal at −50 °C for 5 min and then heated and cooled from −50 to 80 to −50 °C, at a rate of 3 °C min^{-1}, ±0.20 °C amplitude, with a modulation period of 60 s for two continuous cycles. Glass-transition temperature (T_g) was calculated using the tangent intersection method.

Porcine Partial-Thickness Wound Healing Model.

Animal studies were performed in the research animal facility at Children's National Health System. Experiments were approved by the Institutional Animal Care and Use Committee (protocol #30454) and were performed in accordance with the "Guide for the Care and Use of Laboratory Animals" published by the National Institutes of Health. Two 20–25 kg Yorkshire swine were used in this pilot study. Six partial-thickness (0.6 mm depth) skin wounds were made on each side of the paravertebral skin with a dermatome (Humeca), making a total of 12 wounds per animal. The wounds were made 1.5 cm long in the cranial–caudal direction and 4 cm wide. Each wound was separated by 1.5 cm of normal

skin. The wounds were randomized to treatment with either Tegaderm (3M) (a polyurethane-based clinical control), HMW PLCL, or 50:50 L/H, resulting in a total of five wounds per dressing group ($n = 5$) over two animals. Wounds were uniformly sprayed with 2 mL of polymer solution, which produced complete wound coverage as determined by a surgeon. Wounds were assessed daily for healing and signs of infection by visual inspection. Dressing replacement was performed as needed until postwound day (PWD) 14. The experimental end point was chosen to be 35 days after initial wound creation. 5 mm full-thickness punch biopsies of the wounds were also taken on PWDs 3, 7, and 35. Each biopsy was taken from different areas of the same wound.

Histological Analysis.

Biopsied tissues were kept in a 10% neutral-buffered formalin until histological processing (Histoserv Inc.). Punch biopsy samples were bisected along the longitudinal axis and then embedded in paraffin wax. Five micrometer sections were prepared and fixed onto glass slides and then stained with Masson's trichrome. Digital images of the histology slides were taken with TissueScope LE (Huron Digital Pathology) at 40× magnification and then exported for analysis with ImageJ (National Institutes of Health). Images were scaled to 1 μm/pixel. Epidermal and dermal thicknesses were measured after cropping images to 3000 μm by 3000 μm. Epidermis thickness was measured at areas that show at least a basal layer of epidermal cells, stained red in Masson's trichrome. The total dermis thickness was measured from the base of the epidermis to the level of subdermal fat. Also measured was the thickness of the evolving dermal matrix, seen as disorganized collagen bundles (in light blue) above the layer of organized collagen bundles (dark blue). Thickness measurements were taken at the left, middle, and right third of the images and then averaged. The vascular density (vessels per mm^2 of dermis) of each biopsy was measured by counting the number of unique vessel structures in the dermis, including arterioles and venules, but not capillaries. The dermis area was measured using ImageJ. Density measurements were made by two researchers and averaged.

Wound Healing Gene Expression.

Gene expression of α-SMA (α-smooth muscle actin), VEGF (vascular endothelial growth factor), TGF-β1 (transforming growth factor-β1), and collagen I and collagen III in the healed wounds were quantified using real-time reverse transcription-polymerase chain reaction (RT-PCR). Full-thickness biopsies were taken from the center of the healed wounds at PWD 35. Normal uninjured skin biopsies were also taken from both sides of the paraspinal back skin with samples from the upper and lower back. Gene expressions in the wounds were measured relative to those expressed in normal skin tissues. Biopsied tissues were snap-frozen in liquid nitrogen and then stored at −80 °C until analysis.

RNA extraction from the frozen tissue was performed by tissue homogenization in Trizol reagent (Life Technologies) and PureLink RNA Mini Kit (Thermo Fisher Scientific). For all experiments, 3 μg of RNA was used to synthesize the first-strand cDNA using High-Capacity cDNA Reverse Transcription kit (Life Technologies). Real-time PCR was performed using TaqMan Gene Expression Master Mix (Life Technologies) in a QuantStudio 7 Flex Real-Time PCR System (Thermo Fisher Scientific), according to the

manufacturer's instructions. Reactions were performed in triplicate, including no template controls and amplification of a housekeeping gene, GAPDH. Gene-specific assays were Ss03373340_m1 for COL1A1, Ss04245588_m1 for α-SMA, Ss04323768_g1 for COL3A1, Ss03382325_u1 for TGF-β1, and Ss03375629_u1 for GAPDH (Life Technologies). Changes in relative gene expression normalized to GAPDH levels were determined using the ΔΔCt method. The difference between the Ct values (ΔCt) of the gene of interest and the housekeeping gene is calculated for each experimental sample. Then, the difference in the ΔCt values between the experimental and unwounded skin samples ΔΔCt is calculated. The fold-change in expression of the gene of interest between the two samples is then equal to $2^{(-\Delta\Delta Ct)}$.

Adhesive Bandage Pull-Apart Adhesion Testing.

Pull-apart testing was performed on the TA Instruments DMA Q800. CVS Health Plastic One-Size Bandages were placed in baths of ethanol to remove the adhesive. The band-aids were then cut into 8 mm square segments, and the polymer band-aid samples were produced by spraying 2 mL of polymer solution directly onto the smooth surface of the band-aid that was previously coated in the adhesive layer. A bioderived lung sealant (Progel, Beckton Dickinson) constituted of a cross-linked human serum albumin (HSA)–poly(ethylene glycol) (PEG) network or a topical skin adhesive (SwiftSet, Covidien) derived from cyanoacrylate (CA) were used as clinical controls and deposited onto the bandage in an analogous fashion. The band-aid was allowed to set for 15 min in 37 °C ambient air. Square sections of an 8 mm frozen porcine skin were cut and warmed to room temperature by coating the tissue in water and letting the tissue warm for 10 min in a 37 °C ambient air. Prior to testing, porcine skin samples with clinical control as adhesive were coated until the total surface coverage (approximately 250 μL of solution). Warmed polymer-coated band-aids or uncoated band-aids in the case of clinical controls were brought into contact with porcine skin and superglued to the clamps of the dynamic mechanical analyzer in a compression mode, the porcine skin to the fixed clamp and the polymer-coated or uncoated band-aid to the movable clamp. The samples were compressed at 1 N for 5 min, and after this compression period, a controlled force ramp was used to increase the pull-apart force at a rate of 1 N min^{-1} until failure. The adhesion strength of each sample was recorded. Each sample type was replicated five times (n = 5).

Wound Closure Strength Testing.

Wound closure strength testing was performed on the TA Instruments DMA Q800. Sections (1 cm by 1 cm) of the porcine skin were attached to rectangular clamps using cyanoacrylate glue. The rectangular clamps were brought together end to end, and 1 mL of adhesive polymer solution was deposited via SBS on this joint, closing the gap between the two skin-coated clamps (see ASTM F2458–05).[27] The adhesive was carefully applied and trimmed to avoid coating the interface between the ends and edges of the clamps. It was then allowed to set at 37 °C for 10 min before testing. A controlled force ramp was used to increase the force at a rate of 1 N min^{-1} until failure. Failure type was recorded as either adhesive or cohesive. Force values were normalized to the surface area of the skin coated by the adhesive, which was measured using calipers, giving adhesive strength. Each sample type was replicated five times (n = 5).

Statistical Analysis.

Statistical analysis was performed on Origin (OriginLab). Typically, one-way analysis of variance (ANOVA) was used to compare group variation, followed by post hoc pairwise Tukey or Holm–Sidak (for pull-apart adhesion testing) comparisons to determine significant differences between the groups. For adhesion testing, positive and negative controls were excluded from statistical analysis because of differences in variability. Statistical significance is considered for $P < 0.05$. Typically, averages were plotted with error bars representing standard error.

RESULTS

An airbrush was used to deposit polymer fibers directly onto porcine partial-thickness wounds, allowing us to assess the effects of a biodegradable PSA composed of PLCL on wound healing compared to a bandage with a conventional nonbiodegradable adhesive (Figure 1A). Three different pressure-sensitive blends of PLCL were studied (Figure S2), one containing pure high-molecular-weight (HMW) PLCL (Mn 35 000–45 000 Da), one containing a 50:50 blend (50:50 L/H) of HMW PLCL and low-molecular-weight (LMW) PLCL (Mn 15 000–25 000 Da), which acts as a tackifier to enhance adhesion while degrading, and one containing pure LMW PLCL (Figures 1B and S3). Pure adhesive (with no backing) was used in these experiments to isolate the effects of polymer choice. PLCL blends transition from a fibrous covering to a thin, conformal, and transparent film (Figure 2A). We tracked wound dressing changes over the first 14 days of healing to determine how the adhesive affected the frequency at which the dressing had to be replaced (Figure 2B). Both HMW and 50:50 L/H PLCL-based adhesives required fewer dressing changes than the control dressing, Tegaderm, which is a conventional PSA backed with a thin polyurethane film.[28]

Visual assessment of the wounds was regularly performed by a surgeon as they were healing, with pictures presented at postwound days (PWDs) 3, 7, and 21 (Figure 2C–E). Some exudate buildup was apparent underneath the Tegaderm dressing at PWD 3 (Figure 2Ciii). At PWD 21, most wounds appeared to show similar amounts of scarring. While few wounds displayed any healed epidermis at PWD 3, nearly all wounds showed complete epidermis coverage by PWD 7, which was confirmed by histology (Figure 3A).

Increased epidermis thickness was noted in the 50:50 L/H blend at PWD 7 but returned to levels comparable to the other wound dressings at PWD 35 (Figure 3B). Neodermis ratio was significantly lower for HMW PLCL dressings at PWDs 7 and 35 (Figure 3C). Revascularization is an indication of wound healing, as angiogenesis plays a critical role during the proliferative stage of wound repair.[29,30] Blood vessel regeneration was decreased for Tegaderm at PWD 3, while 50:50 L/H displayed increased blood vessel density relative to the no wound control at PWD 7 (Figure 3D). All returned to normal levels at PWD 35. Representative histological images from which these data are compiled are shown from PWD 3 to PWD 35 in Figure 4, and unwounded skin is shown in Figure S1.

Samples were collected from the center of wound at PWDs 3, 7, and 35. Sections were stained with Masson’s trichrome to identify collagen (blue), keratin in the epidermis (dark

red), and blood vessels (red). The overall trajectory of collagen type I and collagen type III mRNA expression over 35 days was similar for all groups (Figure 5A,B), while α smooth muscle actin (α-SMA), transforming growth factor β (TGF-β), and vascular endothelial growth factor (VEGF) were expressed similarly between the three groups (Figure 5C–E). High relative amounts of collagen III, which is disorganized compared to those of collagen I, indicate potential scarring. At day 35, all wound dressing types produce similar type I to type III ratios, although only Tegaderm is significantly lower than unwounded skin (Figure 5F).

After validating the safety and efficacy of using PLCL for use in wound healing applications, we further characterized its adhesive properties and processability toward its eventual use as the adhesive layer on a bandage. PLCL adhesives are sprayable with a tunable fiber morphology, consistently forming a mesh with long fibers at a 50:50 L/H ratio (Figure 6A). The fibers can be sprayed onto various targets and form a thin adhesive film after transitioning (Figure 6B), allowing for simple fabrication. During pull-apart adhesion testing and wound closure strength testing, the film is soft and sticky enough to form tendrils during cohesive failure, indicating the formation of a strong bond (Figure 6C,D).

We sprayed PLCL adhesives onto the backing of a typical plastic bandage (Figure 7A) and compared pull-apart adhesion strength to the same plastic bandage as manufactured, coated with a conventional PSA. After spraying and transitioning, both PLCL adhesives formed a thin film with similar morphology to the conventional adhesive (Figure 7B,C). PLCL has a glass-transition temperature of approximately −11 °C (Figure 7D), which allows it to soften significantly as it warms to body temperature. Pull-apart adhesion strength to porcine skin was significantly greater for both the 50:50 L/H blend of PLCL and Progel control than either pure LMW PLCL or pure HMW PLCL, while the acrylate-based SwiftSet skin adhesive was much greater than all other groups other than conventional bandage PSA (Figure 7E). In wound closure strength testing, the 50:50 L/H blend of PLCL displayed a significant increase compared to that of pure LMW PLCL (Figure 7F). This provides strong evidence in favor of using a combination of tackifying (LMW PLCL) and reinforcing (HMW PLCL) polymers to promote both adhesive and cohesive strength, mimicking the properties of a PSA; 50:50 L/H produces a comparable adhesion strength (12 ± 2 kPa) to Progel control (12 ± 3 kPa) and conventional bandage (11 ± 2 kPa), whose PSA coating has a much lower T_g than PLCL (Figure 7D).

DISCUSSION

Biodegradable and tissue adhesive polymers have been investigated as alternatives to sutures,[31,32] stand-alone wound dressing materials,[25,26,33] and replacements for biomedical devices.[34,35] However, biodegradable polymers have not been investigated as a replacement for conventional pressure-sensitive adhesives in a conventional bandage, one that consists of a flexible backing coated with a thin layer of strong, tacky adhesive. Yet, due to their low cost, ease of use, and availability to consumers, there is a larger market for these simple tapes and bandages than “advanced” wound dressings.[36,37] They are desirable targets for innovation because of the growing body of evidence indicating that the ubiquitous nondegradable PSAs commonly used in them may cause allergic dermatitis. Acrylates,

methacrylates, and phenolic resins that are common in bandage adhesives[38] are implicated in controlled studies of allergic and irritant contact dermatitis.[4,39,40]

We first rigorously characterized the biocompatibility of polyester blends in a partial-thickness wound model, establishing that treated wounds have effective barrier properties (Figure 2), complete dermal and epidermal healing (Figures 3 and 4), and normal biochemical composition (Figure 5). However, for effective translation, a bandage adhesive must also be easily applied as a thin layer on a textile backing during manufacture, stick readily to both the backing and skin, and remain stable at room temperature. The PLCL blends investigated are easily sprayed onto a target (Figure 6A), transition into a thin layer (Figure 6B), and have a desirable balance of cohesive and adhesive strength in pull-apart tests (Figure 6C,D). Furthermore, the layer has a similar morphology to the conventional adhesive layer on a bandage (Figure 7A), with similar thermal properties that allow PLCL blends to soften at room temperature (Figure 7B), and comparable adhesion strength in ex vivo wound closure and pull-apart models (Figure 7E,F). These observations align with previous studies from our group on the pressure-sensitive tissue adhesion of viscoelastic polyester blends.[41] Future studies could validate this approach by employing biodegradable polyesters as adhesives in new wound models and further assessing the biocompatibility with contact dermatitis patch and bandage testing.

CONCLUSIONS

Based on robust preclinical safety data, we have isolated two safe and effective biodegradable polyesters spanning the molecular weight range of interest for developing a strong bonding tissue adhesive that minimizes the need for dressing replacements. We then demonstrated that a 50:50 blend of low- and high-molecular-weight PLCL maximizes adhesion strength. It can also be processed using conventional methods and applied using a typical plastic backing. These polymers could potentially be used safely as a replacement for conventional bandage adhesives with better biocompatibility and comparable adhesion.

Supplementary Material

Refer to Web version on PubMed Central for supplementary material.

ACKNOWLEDGMENTS

The authors acknowledge the support of the Maryland NanoCenter, the AIMLab, the Functional Macromolecular Laboratory, and the Sheikh Zayed Institute for Pediatric Surgical Innovation. Research reported in this publication was supported by the National Institute of Biomedical Imaging and Bioengineering of the National Institutes of Health under Award Number R01EB019963. J.L.D. was supported by the National Institute of Biomedical Imaging and Bioengineering of the National Institutes of Health under Award Number F31EB025735. The content is solely the responsibility of the authors and does not necessarily represent the official views of the National Institutes of Health. S.T.Z. received support from the UMD ASPIRE program.

REFERENCES

(1). Deng X Progress on Rubber-Based Pressure-Sensitive Adhesives. J. Adhes 2018, 94, 77–96.

(2). Shin J; Martello MT; Shrestha M; Wissinger JE; Tolman WB; Hillmyer MA Pressure-Sensitive Adhesives from Renewable Triblock Copolymers. Macromolecules 2011, 44, 87–94.

(3). Falsafi A; Tirrell M; Pocius AV Compositional Effects on the Adhesion of Acrylic Pressure Sensitive Adhesives. Langmuir 2000, 16, 1816–1824.

(4). Widman TJ; Oostman H; Storrs FJ Allergic Contact Dermatitis from MedicalAdhesive Bandages in Patients Who Report Having a Reaction to Medical Bandages. Dermatitis 2008, 19, 32–37. [PubMed: 18346394]

(5). Waring M; Bielfeldt S; Mätzold K; Wilhelm KP; Butcher M An Evaluation of the Skin Stripping of Wound Dressing Adhesives. J. Wound Care 2011, 20, 412–422. [PubMed: 22068140]

(6). Wiegand C; Abel M; Hipler U-C; Elsner P Effect of Non-Adhering Dressings on Promotion of Fibroblast Proliferation and Wound Healing in Vitro. Sci. Rep 2019, 9, No. 4320. [PubMed: 30867534]

(7). Rippon M; White R; Davies P Skin Adhesives and Their Role in Wound Dressings. Wounds UK 2007, 3, 76–86.

(8). King A; Stellar JJ; Blevins A; Shah KN Dressings and Products in Pediatric Wound Care. Adv. Wound Care 2014, 3, 324–334.

(9). Pukki T; Tikkanen M; Halonen S Assessing Mepilex Border in Post-Operative Wound Care. Wounds UK 2010, 6, 30–40.

(10). White R Evidence for Atraumatic Soft Silicone Dressing Use. Wounds UK 2005, 1, 104–109.

(11). Davies P; Rippon M Evidence Review: The Clinical Benefits of Safetac Technology in Wound Care. J. Wound Care 2008, 17, 3–31.

(12). Lantin A; Diegel C; Scheske J; Brönner A; Jodl H Mepilex XT in Practice: Results of a Study in German Specialist Wound Care Centres. Clin. Pract 2016, 7, 4.

(13). Lee BK; Ryu JH; Baek I-B; Kim Y; Jang WI; Kim S-H; Yoon YS; Kim SH; Hong S-G; Byun S; Yu HY Silicone-Based Adhesives with Highly Tunable Adhesion Force for Skin-Contact Applications. Adv. Healthcare Mater. 2017, 6, No. 1700621.

(14). Borde A; Larsson M; Odelberg Y; Hagman J; Löwenhielm P; Larsson A Increased Water Transport in PDMS Silicone Films by Addition of Excipients. Acta Biomater. 2012, 8, 579–588. [PubMed: 22005333]

(15). Mecham S; Sentman A; Sambasivam M Amphiphilic Silicone Copolymers for Pressure Sensitive Adhesive Applications. J. Appl. Polym. Sci 2010, 116, 3265–3270.

(16). Deng W; Lei Y; Zhou S; Zhang A; Lin Y Absorptive Supramolecular Elastomer Wound Dressing Based on Polydimethylsiloxane–(Polyethylene Glycol)–Polydimethylsiloxane Copolymer: Preparation and Characterization. RSC Adv. 2016, 6, 51694–51702.

(17). Nasiri M; Saxon DJ; Reineke TM Enhanced Mechanical and Adhesion Properties in Sustainable Triblock Copolymers via Non-Covalent Interactions. Macromolecules 2018, 51, 2456–2465.

(18). Czech Z; Wilpiszewska K; Tyliszczak B; Jiang X; Bai Y; Shao L Biodegradable Self-Adhesive Tapes with Starch Carrier. Int. J. Adhes. Adhes 2013, 44, 195–199.

(19). Sood A; Granick MS; Tomaselli NL Wound Dressings and Comparative Effectiveness Data. Adv. Wound Care 2014, 3, 511–529.

(20). Narayanan A; Kaur S; Peng C; Debnath D; Mishra K; Liu Q; Dhinojwala A; Joy A Viscosity Attunes the Adhesion of Bioinspired Low Modulus Polyester Adhesive Sealants to Wet Tissues. Biomacromolecules 2019, 20, 2577–2586. [PubMed: 31244021]

(21). Shagan A; Zhang W; Mehta M; Levi S; Kohane DS; Mizrahi B Hot Glue Gun Releasing Biocompatible Tissue Adhesive. Adv. Funct. Mater 2020, 30, No. 1900998.

(22). Daristotle JL; Zaki ST; Lau LW; Torres L; Zografos A; Srinivasan P; Ayyub OB; Sandler AD; Kofinas P Improving the Adhesion, Flexibility, and Hemostatic Efficacy of a Sprayable Polymer Blend Surgical Sealant by Incorporating Silica Particles. Acta Biomater. 2019, 90, 205–216. [PubMed: 30954624]

(23). Zhang W; Ji T; Lyon S; Mehta M; Zheng Y; Deng X; Liu A; Shagan A; Mizrahi B; Kohane DS Functionalized Multiarmed Polycaprolactones as Biocompatible Tissue Adhesives. ACS Appl. Mater. Interfaces 2020, 12, 17314–17320. [PubMed: 32227980]

(24). Cohn D; Lando G Tailoring Lactide/Caprolactone Co-Oligomers as Tissue Adhesives. Biomaterials 2004, 25, 5875–5884. [PubMed: 15172500]

(25). Behrens AM; Casey BJ; Sikorski MJ; Wu KL; Tutak W; Sandler AD; Kofinas P In Situ Deposition of PLGA Nanofibers via Solution Blow Spinning. ACS Macro Lett. 2014, 3, 249–254.

(26). Daristotle JL; Lau LW; Erdi M; Hunter J; Djoum A; Srinivasan P; Wu X; Basu M; Ayyub OB; Sandler AD; Kofinas P Sprayable and Biodegradable, Intrinsically Adhesive Wound Dressing with Antimicrobial Properties. Bioeng. Transl. Med 2020, 5, No. e10149. [PubMed: 31989038]

(27). Subcommittee F04.05. Standard Test Method for Wound Closure Strength of Tissue Adhesives and Sealants; ASTM F2458; ASTM International, 2015. 10.1520/F2458-05R15.

(28). Barnett A; Berkowitz RL; Mills R; Vistnes LM Comparison of Synthetic Adhesive Moisture Vapor Permeable and Fine Mesh Gauze Dressings for Split-Thickness Skin Graft Donor Sites. Am. J. Surg 1983, 145, 379–381. [PubMed: 6340546]

(29). Gurtner GC; Werner S; Barrandon Y; Longaker MT Wound Repair and Regeneration. Nature 2008, 453, 314–321. [PubMed: 18480812]

(30). Li J; Zhang Y-P; Kirsner RS Angiogenesis in Wound Repair: Angiogenic Growth Factors and the Extracellular Matrix. Microsc. Res. Tech 2003, 60, 107–114. [PubMed: 12500267]

(31). Behrens AM; Lee NG; Casey BJ; Srinivasan P; Sikorski MJ; Daristotle JL; Sandler AD; Kofinas P Biodegradable-Polymer-Blend-Based Surgical Sealant with Body-Temperature-Mediated Adhesion. Adv. Mater 2015, 27, 8056–8061. [PubMed: 26554545]

(32). Kern NG; Behrens AM; Srinivasan P; Rossi CT; Daristotle JL; Kofinas P; Sandler AD Solution Blow Spun Polymer: A Novel Preclinical Surgical Sealant for Bowel Anastomoses. J. Pediatr. Surg 2017, 52, 1308–1312. [PubMed: 27956071]

(33). Wang W; Liu S; Chen B; Yan X; Li S; Ma X; Yu X DNA-Inspired Adhesive Hydrogels Based on the Biodegradable Polyphosphoesters Tackified by a Nucleobase. Biomacromolecules 2019, 20, 3672–3683. [PubMed: 31513395]

(34). Kim HJ; Choi B-H; Jun SH; Cha HJ Sandcastle Worm-Inspired Blood-Resistant Bone Graft Binder Using a Sticky Mussel Protein for Augmented In Vivo Bone Regeneration. Adv. Healthcare Mater 2016, 5, 3191–3202.

(35). Lang N; Pereira MJ; Lee Y; Friehs I; Vasilyev NV; Feins EN; Ablasser K; O'Cearbhaill ED; Xu C; Fabozzo A; Padera R; Wasserman S; Freudenthal F; Ferreira LS; Langer R; Karp JM; del Nido PJ A Blood-Resistant Surgical Glue for Minimally Invasive Repair of Vessels and Heart Defects. Sci. Transl. Med 2014, 6, No. 218ra6.

(36). Grand View Research. Advanced Wound Dressing Market Size, Share & Trends Report, 2026, GVR-2–68038-980–7; 2019.

(37). Grand View Research. Medical Tapes and Bandages Market Size|Industry Report, 2018–2025, GVR-2–68038-259–4; 2017.

(38). Tam I; Wang JX; De J Identifying Acrylates in Medical Adhesives. Dermatitis 2020, 31, e40–e42. [PubMed: 32665520]

(39). Spencer A; Gazzani P; Thompson DA Acrylate and Methacrylate Contact Allergy and Allergic Contact Disease: A 13-Year Review. Contact Dermatitis 2016, 75, 157–164. [PubMed: 27402324]

(40). Norris P; Storrs FJ Allergic Contact Dermatitis to Adhesive Bandages. Dermatol. Clin 1990, 8, 147–152. [PubMed: 2302854]

(41). Daristotle JL; Zaki ST; Lau LW; Ayyub OB; Djouini M; Srinivasan P; Erdi M; Sandler AD; Kofinas P Pressure-Sensitive Tissue Adhesion and Biodegradation of Viscoelastic Polymer Blends. ACS Appl. Mater. Interfaces 2020, 12, 16050–16057. [PubMed: 32191429]

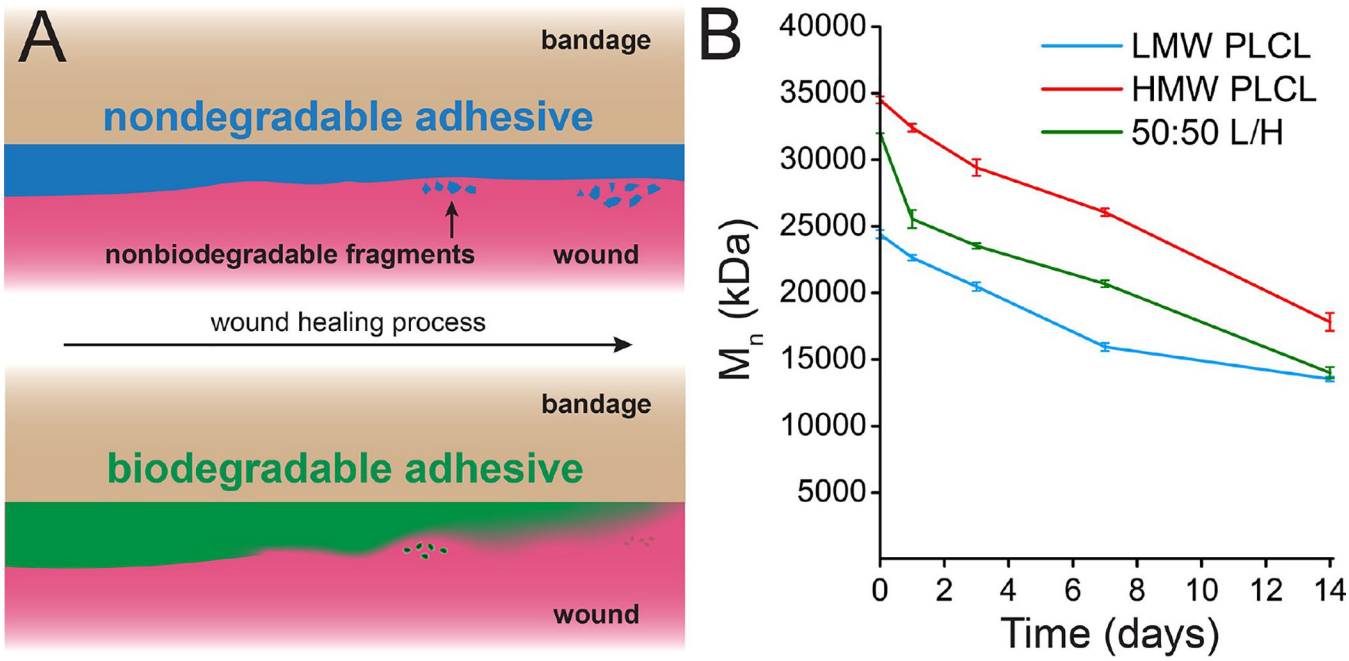

Figure 1.

(A) While the adhesive on a conventional bandage may produce nonbiodegradable fragments that irritate the skin, a biodegradable adhesive can degrade into absorbable monomers. (B) Gel permeation chromatography of low-molecular-weight (LMW) poly(lactide-*co*-caprolactone) (PLCL), high-molecular-weight PLCL, and a 50:50 blend of those two polymers (50:50 L/H), which has pressure-sensitive adhesive properties, during in vitro degradation.

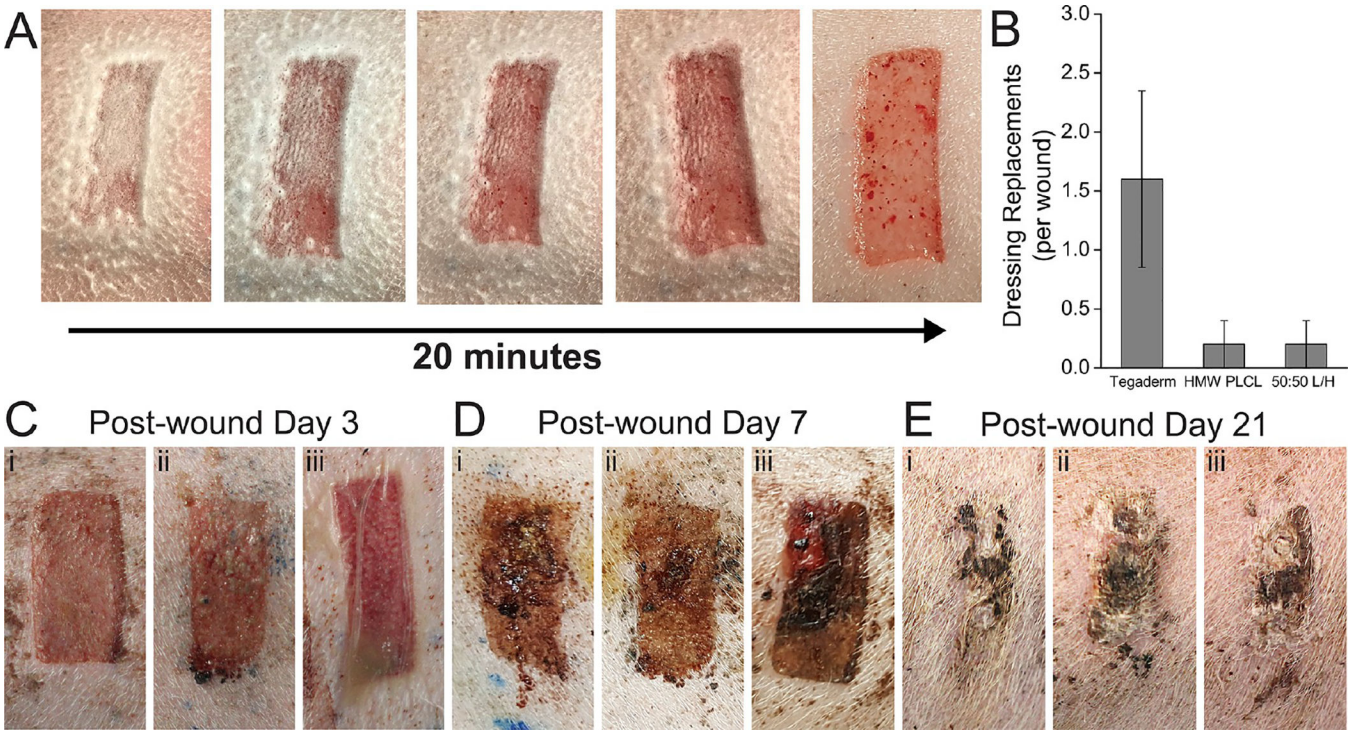

Figure 2.

(A) Partial-thickness wound sprayed with a PLCL blend pressure-sensitive adhesive, transitioning from solution blow spun fibers to a transparent film. (B) Number of required dressing replacements per wound due to dressing deadherence. Sample images of healing wounds at (C) 3 days, (D) 7 days, and (E) 21 days after wound creation, using either (i) HMW PLCL, (ii) 50:50 L/H PLCL, or (iii) Tegaderm.

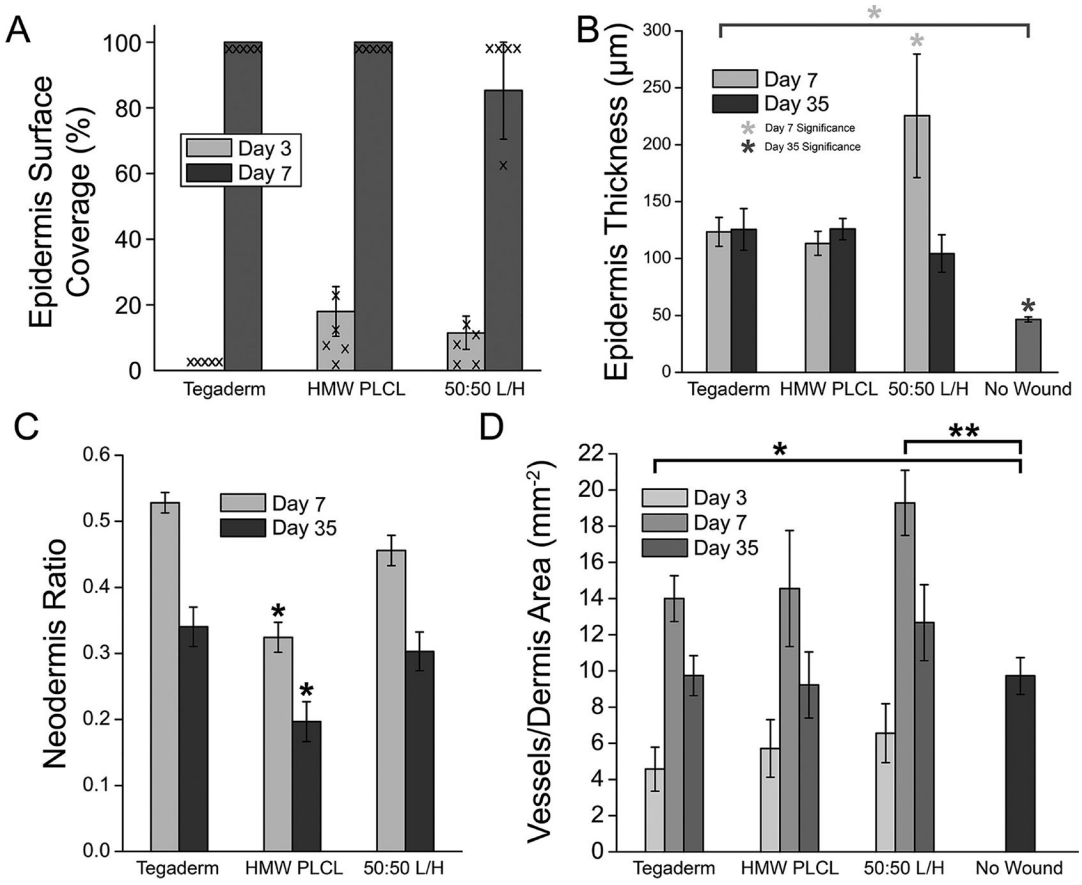

Figure 3.

Histological characteristics of partial-thickness wound healing for PLCL-based pressure-sensitive adhesives. (A) Epidermis surface coverage on the healing wound at days 3 and 7. Individual data points are overlaid. (B) Epidermis thickness of the healing wounds. (C) Ratio of neodermis thickness to total dermis thickness. (D) Blood vessel density in the dermis of the healing wound. Asterisks indicate statistical significance: * $P<0.05$, ** $P<0.01$.

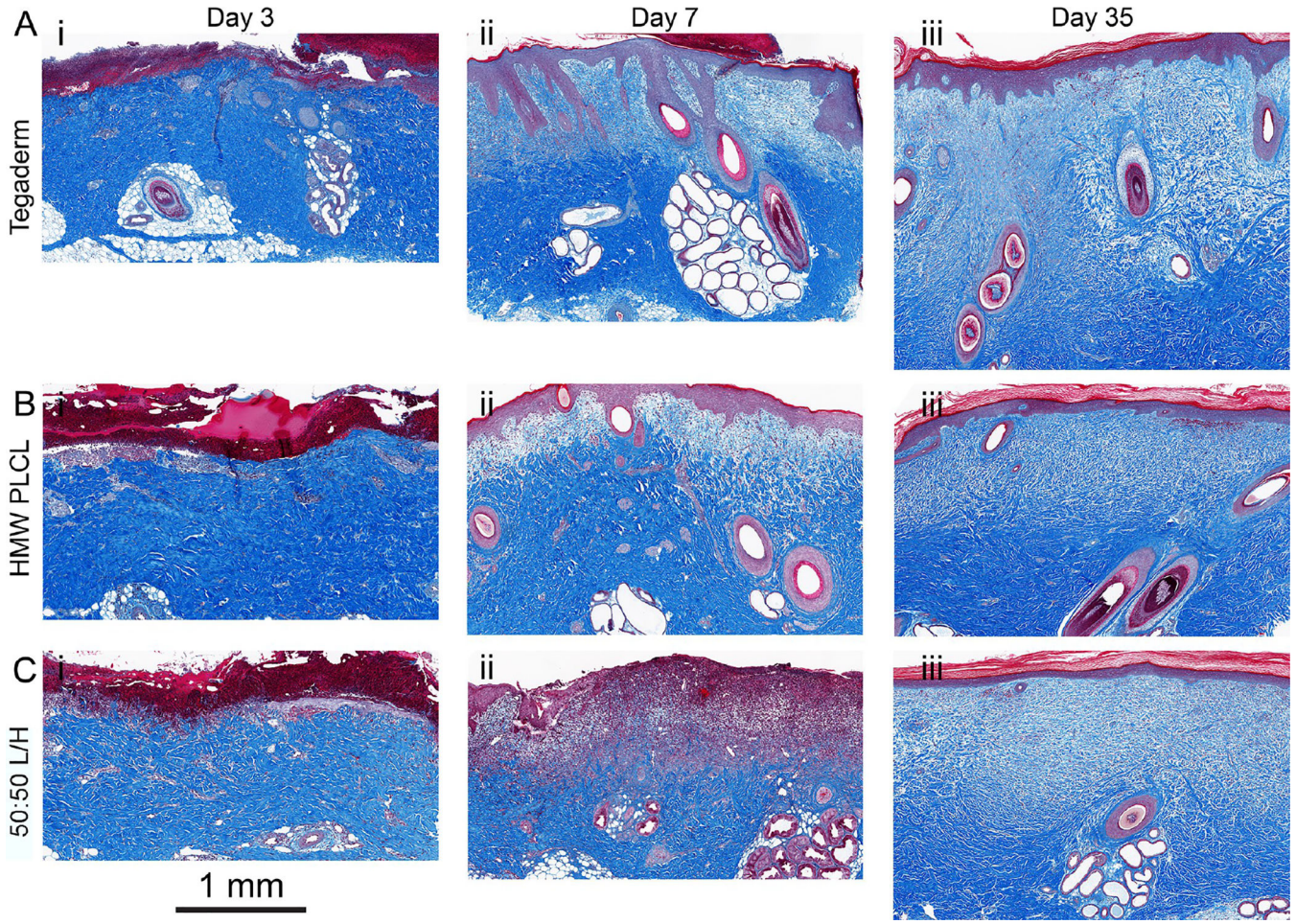

Figure 4.

Representative histological images at postwound days 3, 7, and 35 from porcine partial-thickness wounds sealed with (A) Tegaderm, (B) HMW PLCL, and (C) 50:50 L/H. Each time series of images is from one wound.

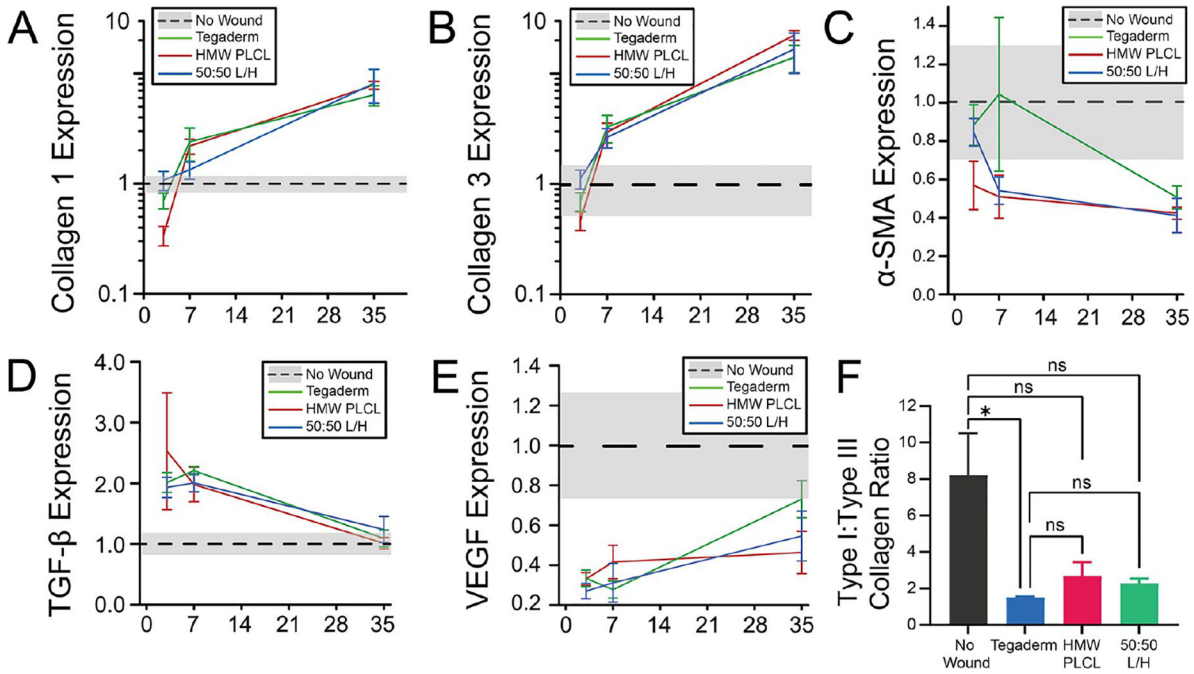

Figure 5.

RT-PCR measurements of (A) collagen I, (B) collagen III, (C) α-SMA, (D) TGF-β, and (E) VEGF. Gene expression measured relative to those of the normal uninjured (no wound) skin, which is plotted with a black dotted line and a gray band indicating standard error. (F) Collagen type I to collagen type III ratio at day 35. * $P < 0.05$.

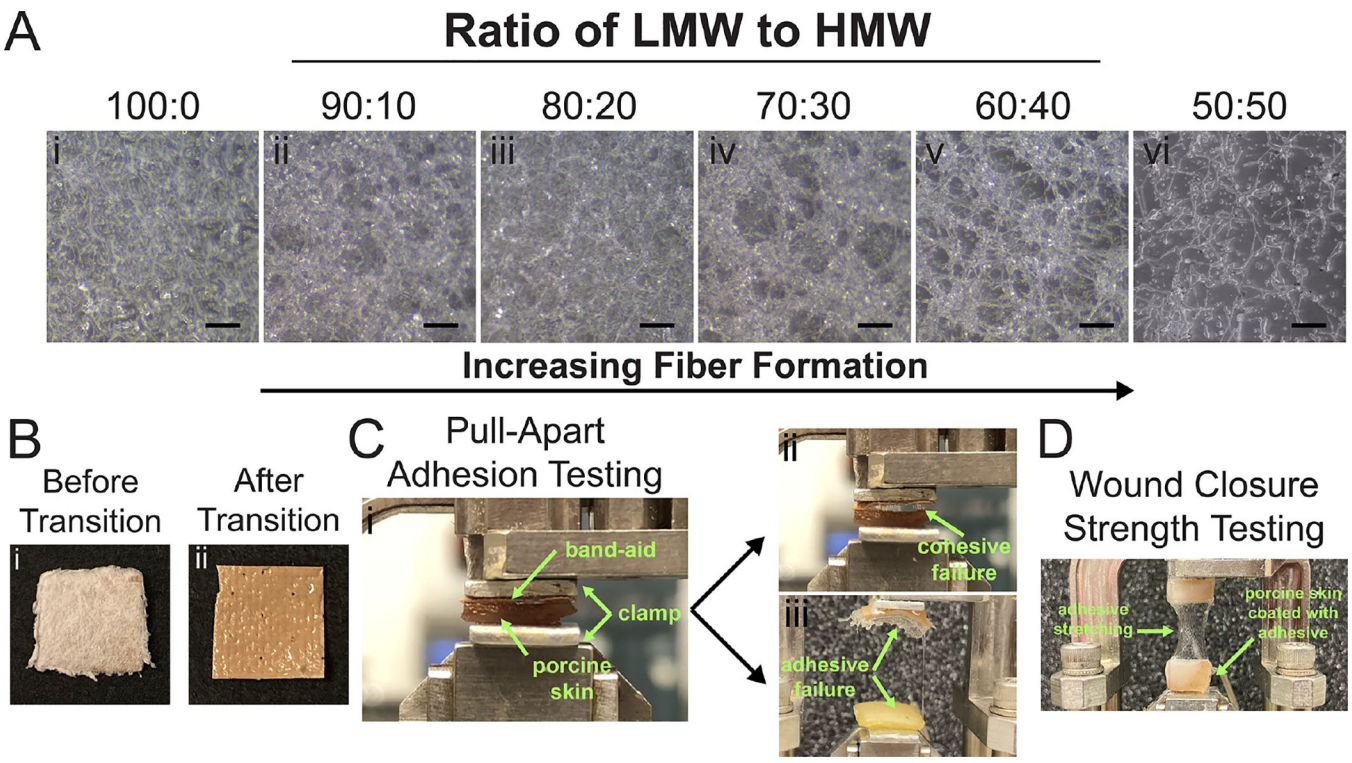

Figure 6.

(A) When more HMW PLCL is incorporated, fiber mats are produced by solution blow spinning from an airbrush. (B) PLCL blends transition from fibers to a thin, adhesive film after 30 minutes. (C) During pull-apart adhesion testing, the adhesive stretches and breaks via cohesive or adhesive failure (green arrows). (D) Wound closure strength test with shear force applied to the joint.

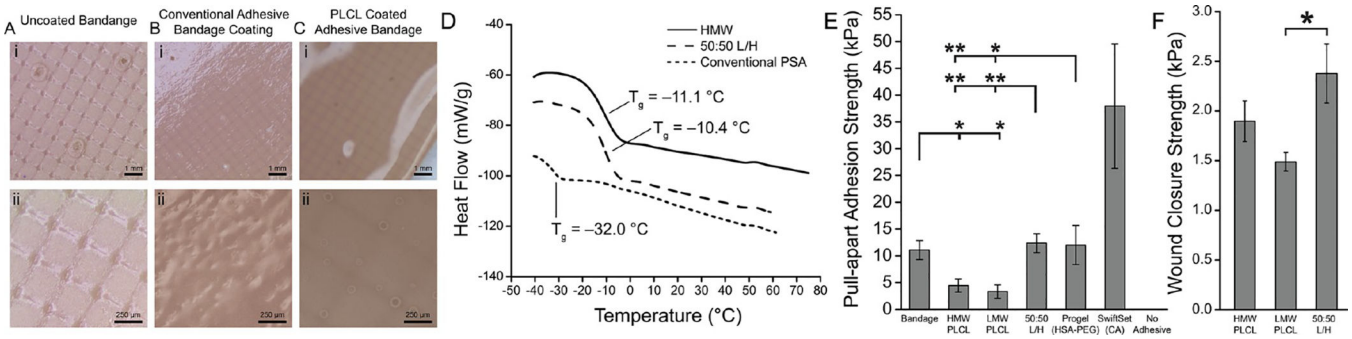

Figure 7.

Biodegradable PLCL pressure-sensitive adhesives were sprayed onto plastic bandages, producing comparable adhesive strength to a conventional polybutylene pressure-sensitive adhesive. Optical microscopy of (A) an uncoated plastic bandage, (B) a plastic bandage coated with a conventional pressure-sensitive adhesive (PSA), and (C) a plastic bandage coated with a PLCL blend adhesive. (D) Differential scanning calorimetry of HMW PLCL, PLCL blend adhesive, and conventional PSA utilized with band-aid. (E) Pull-apart adhesion strength between bandage and porcine skin for neat and blended PLCL, conventional bandage PSA, Progel lung sealant (HSA-PEG), and SwiftSet topical skin adhesive (CA). (F) Wound closure strength of PLCL 50:50 L/H blend compared to those of pure LMW and HMW polymers. Asterisks indicate statistical significance: * $P < 0.05$, ** $P < 0.01$.